J Neurol (2008) 255:575–580
DOI 10.1007/s00415-008-0751-8

ORIGINAL COMMUNICATION

Maria-João Ribeiro
Ahmed Idbaih
Caroline Thomas
Philippe Remy
Nadine Martin-Duverneuil
Yves Samson
Jean Donadieu
Khê Hoang-Xuan

^{18}F-FDG PET in neurodegenerative Langerhans cell histiocytosis

Results and potential interest for an early diagnosis of the disease

Received: 11 August 2006
Received in revised form: 16 May 2007
Accepted: 19 September 2007
Published online: 31 January 2008

M.-J. Ribeiro MD, PhD (✉)
Service Hospitalier Frédéric Joliot
DRM/DSV, CEA
4, place du Général Leclerc
91406 Orsay, France
Tel.: +33 1 69 86 78 00
Fax: +33 1 69 86 77 28
E-Mail: maria-joao.ribeiro@cea.fr

A. Idbaih MD, PhD ·
K. Hoang-Xuan MD, PhD
Service de Neurologie Mazarin, AP-HP
Groupe Hospitalier Pitié-Salpêtrière
UPMC, Paris, France

C. Thomas MD
Unité d'Hématologie et d'Oncologie Pédiatrique
CHU, Nantes, France

P. Remy MD, PhD
URA-CNRS-CEA 2210
Service Hospitalier Frédéric Joliot
Orsay, France

P. Remy MD, PhD
Département de Neurosciences, AP-HP
CHU Henri Mondor
Faculté de Médecine Paris XII
Créteil, France

N. Martin-Duverneuil MD
Service de Neuroradiologie, AP-HP
Groupe Hospitalier Pitié-Salpêtrière
UPM, Paris, France

Y. Samson MD
Urgences Cérébro-Vasculaires, AP-HP
Groupe Hospitalier Pitié-Salpêtrière
Paris, France

J. Donadieu MD, PhD
Service d'Hématologie et d'Oncologie Pédiatrique, AP-HP
Hôpital d'Enfants Armand Trousseau
Paris, France

Abstract *Introduction* The so called "neurodegenerative Langerhans cell histiocytosis" (ND-LCH) is a rare and severe complication of LCH presenting as a progressive cerebellar ataxia associated with pyramidal tract signs, and cognitive impairment. MRI is the gold standard to investigate CNS lesions of ND-LCH but little is known about functional changes observed in this disease. *Objectives* To search for CNS metabolic changes in ND-LCH. *Methods* Seven patients suffering from ND-LCH were investigated by ^{18}F-FDG PET in this prospective study and compared with 21 healthy controls. *Results* ND-LCH patients demonstrated recurrent abnormalities including bilateral hypometabolism in the cerebellum, the basal ganglia (caudate nuclei), frontal cortex and, bilateral, a relatively increased metabolism in the amygdalae ($p < 0.001$). Functional changes in these anatomical regions may be detected in the absence of any apparent lesion on MRI. *Conclusions* ND-LCH demonstrates a recurrent ^{18}F-FDG PET metabolic signature. Our results suggest that ^{18}F-FDG PET might be a useful tool for an early diagnosis of ND-LCH before neuroradiologic abnormalities appear.

Key words Langerhans cell histiocytosis · neurodegenerative Langerhans cell histiocytosis CNS · ^{18}F-FDG PET

Introduction

Langerhans cell histiocytosis (LCH), formerly known as histiocytosis X, is a rare multisystemic disease characterized by a clonal proliferation of Langerhans cells. This disease may involve all organs particularly skull bones, skin, the hypothalamo-pituitary axis and the ears/nose/throat. The clinical presentation of the disease is heterogeneous ranging from a solitary eosinophilic granuloma of the bone to a multisystemic disease with severe organ failure [1].

CNS involvement or neuro-LCH occurs in about 5 to 10 % of cases [2]. Excluding hypothalamo-pituitary axis involvement, neurohistiocytosis is classified as either the (1) tumor-like form or (2) the neurodegenerative-like form, according to the clinical and neuroradiological presentation. Rarely, both forms may be present in the same patient.

The tumor-like form is the better known subtype of

JON 2751

neuro-LCH. CNS involvement is revealed by seizures or focal site-dependent signs. It is characterized on MRI by one or multiple space occupying lesions strongly enhanced by contrast. Complete remission is often obtained by surgery when the lesion is unique and accessible. Chemotherapy may represent an alternative for multiple lesions or inoperable lesions [3]. Pathological features of tumor-like lesions reveal typical proliferation of LCH cells.

The neurodegenerative form (ND-LCH) is less understood. Patients develop a progressive cerebellar ataxia frequently associated in the course of the disease with pyramidal tract signs, pseudobulbar palsy and cognitive impairment. MRI classically reveals a "cockade aspect" of the cerebellum (high T2 signal of the corpus medullare and high T1 signal of dentate nuclei) associated with a symmetrical hypersignal on T1-weighted images of the globus pallidus [4–7]. However the MRI may be normal or show only discrete cerebellar atrophy. Neuropathological studies of ND-LCH are scarce, showing in most cases demyelination, neuronal loss, gliosis, more rarely inflammatory infiltrates [8] but no infiltration by CD1a LCH cells [8]. To date, no treatment has been shown to improve the clinical course of the disease and the neuroradiological lesions [4]. The diagnosis may be difficult especially when the neurological signs are the presenting symptoms of the disease and the MRI is normal or shows nonspecific lesions. Altogether, degenerative-like lesions of neuro-LCH raise many unresolved pathophysiological questions [9, 10].

In order to evaluate the pattern of cerebral metabolic abnormalities, seven patients with ND-LCH were studied by brain magnetic resonance imaging (MRI) and positron emission tomography (PET) using fluorodeoxyglucose labelled with fluorine 18 (^{18}F-FDG).

Methods

Patients

Four men and three women, 14 to 66 years of age at inclusion (median age 19 years) with ND-LCH (Table 1) were studied with MRI and ^{18}F-FDG PET. The patients were selected based on a pathologically confirmed systemic LCH. One patient did not meet the full criteria of DN-LCH (lack of pathological confirmation) but was nonetheless enrolled because all other diagnoses had been ruled out and the patient presented progressive ataxia, diabetes insipidus and typical MRI features of DN-LCH [5]. CNS adverse effects of medical treatments received previously were ruled out; particularly the patients did not receive CNS radiotherapy or methotrexate-based chemotherapy.

The patients were compared to 21 healthy subjects (12 men, 9 women), 23 to 50 years old (median age 35 years) previously studied with ^{18}F-FDG. None of these controls had neurological history, clinical abnormality, or abnormal findings on brain MRI. The ongoing protocols in our centers (Salpêtrière-Paris Hospital or CEA-Orsay, France) were approved by the local ethics committee, and each subject (or their parents if a minor) gave a written informed consent.

MRI and PET acquisitions

Brain MRI was obtained for all subjects using a 1.5 Tesla imager (Signa, General Electric). T2-weighted images from each subject were used to identify white matter lesions. In addition, a T1-weighted in-

Table 1 Main clinical and neuroradiological characteristics of the seven patients

Patient	Age/Sex (years)	Disease onset (years)	Systemic involvement	Treatments prior CNS involvement	Age at onset of first neurological signs (years)	Neurological signs	Neuroradiological signs on MRI
1	67/M	43	Skin, stomatologic, ENT, liver, brain	Topical mechlorethamine	64	Cerebellar ataxia, pyramidal signs	Cerebellar atrophy
2	18/F	17	Lungs, brain	Vinblastin, steroid therapy, purinethol	17	Cerebellar ataxia, pyramidal signs	Periventricular, cerebellar white matter, dentate nuclei and globus pallidus changes
3	21/F	11	Diabetes insipidus, brain	None	17	Cerebellar ataxia, pyramidal signs, dystonia pseudobulbar palsy	Cerebellar white matter, dentate nuclei and globus pallidus changes
4	18/F	2.5	Skin, lungs, skull, ENT, GH deficiency, brain	Vinblastin, steroid therapy	6	Cerebellar ataxia	Supratentorial white matter, globus pallidus and dentate nuclei changes
5	24/M	0.8	Skeleton, brain, GH deficiency	None	20	Cerebellar ataxia, pyramidal signs	Cerebellar white matter and dentate nuclei changes
6	17/F	1.8	Skin, brain	Topical mechlorethamine	2	Cerebellar ataxia, pyramidal signs, cognitive impairment	Cerebellar and brainstem atrophy
7	19/M	9	Skeleton, diabetes insipidus, GH deficiency, brain	None	11	Cerebellar ataxia cognitive impairment, pyramidal signs	Cerebellar white matter changes

ENT ear nose throat; *GH* growth hormone

version recovery spoiled gradient (SPGR) acquisition was performed to allow a 3D reconstruction of MR images to perform the co-registration between PET and MRI. The volume based co-registration of MRI and PET images was performed using mutual information as matching criterion [11]. Global rigid transformation was considered for the spatial alignment [12].

PET studies were performed using ECAT EXACT HR+ (Siemens Medical Solutions) which collects 63 simultaneous 2.4 mm-thick slices, having an intrinsic in-plane resolution of 4.3 mm. The subjects were positioned in the scanner using three-dimensional laser alignment. A thermoplastic head mask was molded to each subject's face to restrain head movements. Tissue attenuation was measured before radiotracer administration using three rod sources of ^{68}Ge. ^{18}F-FDG was injected intravenously with a mean dose of 148 MBq. Image acquisition in 3D mode was started 30 minutes after ^{18}F-FDG injection and ended 20 minutes later.

Image analysis

In order to detect abnormal ^{18}F-FDG uptake, patient individual images were analyzed by visual inspection.

^{18}F-FDG PET images were also analyzed using Statistical Parametric Mapping software (SPM 99, Wellcome Department of Cognitive Neurology, University College, London, UK). After realignment, all images were transformed into a standardized space. This spatial transformation matches each set of images to a template image conformed to the Talairach space. In order to improve the signal to noise ratio, images were smoothed with an 8 mm full-width half-maximum isotropic Gaussian kernel. Global variance was removed by proportional scaling. The SPM comparison between groups was performed using the *t* statistic test further transformed into statistic (SPM [Z]) maps. The two groups (7 patients with ND-LCH *vs* 21 normal subjects) were compared using a *t* test analysis and the changes were considered significant at the $p < 0.001$ level.

Results

The main clinical and MRI findings are summarized in Table 1.

Individual PET imaging analysis

Patient 1: several foci of decreased ^{18}F-FDG uptake in the left caudate nucleus, the right thalamus, the frontal cortex and the cerebellum (vermis) and relatively increased uptake of the radiotracer in the left amygdala and in the right hippocampus.

Patient 2: small area over the left putamen and both left and right caudate nuclei presenting a decreased uptake of ^{18}F-FDG and a focus of relatively increased uptake of the ^{18}F-FDG in the right amygdala.

Patient 3: decreased ^{18}F-FDG uptake in the left putamen, bilateral in the caudate nuclei, the cerebellum (Fig. 1) and a relatively increased uptake of the radiotracer in both amygdalae and in the left cerebellar lobe; an also important cortical hypometabolism.

Patient 4: decreased radiotracer uptake in the vermis, the left putamen and both caudate nuclei with a relatively small increased focus over the right putamen.

Patient 5: two hypometabolic spots in the cerebellar lobe with a small decreased uptake of ^{18}F-FDG in the right caudate nucleus and the left putamen associated with a slightly and relatively increased uptake of the ^{18}F-FDG in the right amygdala.

Patient 6: hypometabolism of the vermis; heterogeneous metabolism in the frontal and temporal cortex and a focus of decreased uptake of ^{18}F-FDG in the left caudate nucleus.

Patient 7: hypometabolism of the cerebellum; small focus of increased ^{18}F-FDG uptake in the right temporal cortex and decreased ^{18}F-FDG uptake focus in the left frontal cortex.

SPM analysis

SPM analysis revealed a significant decrease ($p < 0.001$) of the ^{18}F-FDG uptake in several regions (Table 2a, Fig. 2) corresponding to cerebral hypometabolism. In Table 2b and Fig. 2, we show the different foci presenting a relatively increased uptake of ^{18}F-FDG ($p < 0.001$) which could correspond to hypermetabolism of these regions.

Discussion

Little is known about CNS functional changes in LCH [13]. Brain imaging with PET after ^{18}F-FDG administration provides information on metabolic CNS involvement by detecting areas of abnormal hypo- or hypermetabolism, which represent functional data not

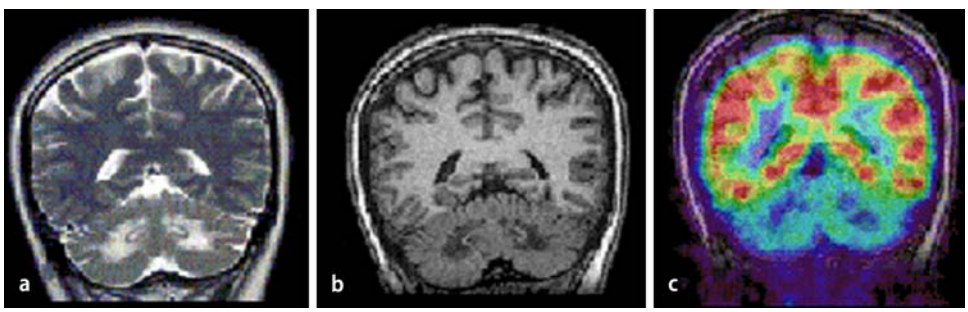

Fig. 1 Example of MRI and PET images obtained for one patient (patient 3). Coronal T2-weighted (**a**) and T1-weighted SPGR (**b**) MRI images. Co-registered coronal T1-weighted SPGR MRI with coronal ^{18}F-FDG (**c**). MRI images show a high T2 signal of the corpus medullae and a high T1 signal of dentate nuclei. For this patient, the co-registered image shows a decreased uptake of the radiotracer by the cerebellum

Table 2a Brain regions associated with significant hypometabolism ($p < 0.001$)

Region	Talairach coordinates			Z score	Voxel number
	x	y	z		
Caudate nucleus R	14	12	10	5.66	299
Caudate nucleus L	−14	6	16	5.49	224
Putamen L	−26	6	6	5.12	363
Inferior frontal gyrus (BA 44) R	52	16	10	5.57	165
Precentralis gyrus (motor cortex) (BA 4) R	42	−18	40	5.45	408
Middle frontal gyrus (BA 10) R	32	48	10	5.38	367
Middle frontal gyrus (BA 47) R	34	34	−12	5.22	199
Middle frontal gyrus (BA 8) R	30	12	50	4.27	136
Middle fontal gyrus (BA 46) L	−30	34	22	4.59	129
Middle frontal gyrus (BA 10) L	−44	50	6	4.52	122
Cerebellum (vermis)	−2	−40	−12	4.15	172

1 voxel = 8 mm^3, *R* right, *L* left

Table 2b Brain regions associated with relatively significant hypermetabolism ($p < 0.001$)

Anatomical region	Talairach Coordinates			Z score	Voxel number
	x	y	z		
Amygdala R	24	−6	−12	6.24	1498
Amygdala L	−10	−8	−14	5.72	1383
Cingulate and frontal gyrus L	−12	−8	40	4.92	291

1 voxel = 8 mm^3, *R* right, *L* left

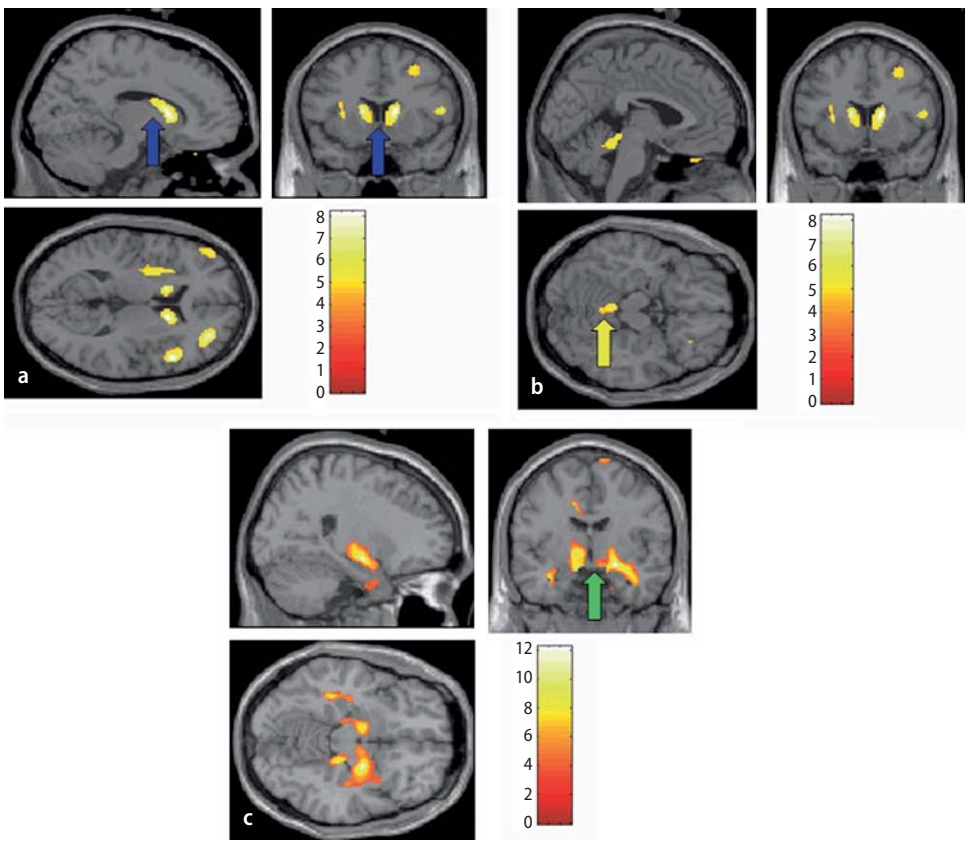

Fig. 2 Group analysis using statistical parametric mapping. The significant results of this analysis ($p < 0.001$) are shown using an overlay on a single subject MRI. Cerebral regions with significant hypometabolism; blue arrow: caudate nuclei (**a**); yellow arrow: vermis of the cerebellum (**b**). Cerebral regions (including amygdalae: green arrow) presenting a relative hypermetabolism (**c**)

available from anatomical imaging methods. To our knowledge, the present PET study is the first specifically devoted to patients suffering from pure ND-LCH.

We showed that ND-LCH patients revealed recurrent functional abnormalities. Bilateral decreased ^{18}F-FDG uptake was observed in basal ganglia especially in the caudate nuclei (6/7 patients), in the cerebellum (especially in the vermis) (6/7 patients) and in the cerebral cortex (fronto temporal cortex) (5/7 patients). Areas of hypometabolism likely reflect neuronal loss and neurodegenerative lesions classically described in ND-LCH [10, 14–16]. While the functional changes detected with PET in the cerebellum were well correlated with the presence of lesions on MRI (all the patients had cerebellar white matter damage or cerebellar atrophy), only 3/6 patients with decreased uptake in the caudate nuclei and 0/4 in the frontal cortex had detectable abnormalities in these anatomical regions on MRI. In addition to abnormal hypometabolism, bilateral but relatively increased uptake of ^{18}F-FDG was also detected, but restricted to the amygdalae in 4/7 patients. Interestingly, this feature was shared by the 4 patients of the present series who had the shortest duration of neurological disease. Since this latter region did not show any abnormalities on MRI, hypermetabolism might represent an early compensatory mechanism which will disappear in the course of the disease, rather than an active ongoing disease process. On the other hand, this apparent hypermetabolism could be an artifact due to the global scaling used. This possibility appears to be most likely because of the absence of corresponding symptoms. In fact, in systemic diseases with potentially widespread abnormalities, metabolism of normal brain regions may appear "increased", whereas mildly impaired brain regions may appear normal (which does not prove that they are normal). However the most impaired regions will appear decreased.

Despite some drugs being able to induce neurological signs and modification of CNS glucose uptake during LCH evolution, the neurological manifestations observed were not induced by therapy in our series. Indeed, only 2/7 patients received systemic chemotherapy before the apparition of neurological signs. The ^{18}F-FDG PET pattern described is then related to ND-LCH and not to drug therapy toxicity.

^{18}F-FDG PET studies investigating CNS in LCH are scarce, and to our knowledge the data of only two patients suffering from ND-LCH have been detailed in the literature. Calming *et al.* reported a series of 7 LCH patients with neurological complications. However, only one patient fulfilled the criteria of ND-LCH. This 18-year old man developed ataxia and spasticity seven years after the diagnosis of LCH. A decreased uptake in the basal ganglia, the hypothalamus, and the cerebellum was found. All other patients of this study had diabetes insipidus (DI) as the single clinical manifestation or in combination with an active hypothalamic mass lesion. The patients with an isolated DI showed a decreased uptake in the hypothalamus (3/3 patients); in contrast, patients with granulomas displayed an increased uptake in the hypothalamus (2/3 patients). Manning et al. [17] reported a single case of a 69 year old woman who presented a ND-LCH associated with an hypothalamic mass lesion. Interestingly, apart from hypothalamic hypermetabolism corresponding to the site of the granulomatous active process, the patient also displayed hypometabolism involving the caudate nuclei and small regions in the fronto-parietal cortex [17]. Altogether, our results confirm to a larger extent the functional involvement in ND-LCH of the cerebellum, but also and this was less expected, the frequent involvement of the basal ganglia, especially the caudate nuclei, the frontal cortex, and the amygdalae. This may at least partly explain some cognitive deficits such as slow processing speed, short-term memory, executive and attentional dysfunctions which have been displayed in ND-LCH (personal data) [14, 18, 19]. The diagnosis and extent of neuro-LCH are usually assessed by clinical examination and conventional neuroimaging. MRI, more sensitive than CT to detect white and grey matter abnormalities, represents currently the gold standard [8–10]. The diagnosis of ND-LCH is easy when the LCH disease is already known and when the MRI demonstrates a typical presentation [4]. However, the suggestive neuroradiological signature is not constant and the MRI may be normal or show only subtle and nonspecific abnormalities (as illustrated by patient 2); moreover the CNS may be the initial location of the disease. Hence, PET although not completely specific (similar decreased uptake in the basal ganglia especially in the caudate nuclei, in the putamen and in the cortex have been also reported in other neurodegenerative diseases such as multiple systemic atrophy [20] and progressive supranuclear palsy [21]) in addition to MRI may be helpful to support the diagnosis of ND-LCH in difficult or atypical cases. Since metabolic changes probably precede MRI lesions, PET might also represent a useful non-invasive tool to diagnose ND-LCH at an early stage, before neuroradiologic abnormalities appear. We have recently showed that patients who develop endocrine LCH disorders, especially diabetes insipidus, are exposed to a high risk of ND-LCH and require long-term follow-up [1]. Therefore these patients also represent good candidates to be investigated longitudinally by PET [22]. Finally, PET might be a very sensitive method to assess the initial extent of the CNS disease and monitor therapy in future trials.

In conclusion, our results suggest that ^{18}F-FDG PET is of interest in ND-LCH: [1] it may be helpful for the diagnosis of atypical cases in addition to MRI, [2] it allows a better assessment of the extent of the CNS disease, and [3] it may contribute to a better understanding of the clinical symptoms and the pathophysiology of the dis-

ease which remain largely unknown. Further studies are warranted to evaluate ^{18}F-FDG PET as a potential sensitive method for an early detection and follow-up of ND-LCH patients or LCH patients with high risk to develop ND-LCH.

Acknowledgements We are greatly indebted to the nursing staff of Service Hospitalier Frédéric Joliot, Orsay, France for patient management. We thank the clinical staff from the several hospital centers participants in this study: Dr T. Généreau (Nantes), Dr Minier (CH Chalon sur Saone), Dr Piguet (CH Limoges), the French Langerhans Hystiocytosis Study Group and the ANR GIS Maladies rares/EPILCH 2005. This work is supported by a grant GIS maladies rares/EPI-LCH 2005.

References

1. Donadieu J, Rolon MA, Thomas C, et al. (2004) Endocrine involvement in pediatric-onset Langerhans' cell histiocytosis: a population-based study. J Pediatr 144:344–350
2. The French Langerhans' Cell Histiocytosis Study Group (1996) A multicentre retrospective survey of Langerhans' cell histiocytosis: 348 cases observed between 1983 and 1993. Arch Dis Child 75:17–24
3. Carpentier MA, Maheut J, Grangeponte MC, Billard C, Santini JJ (1991) Disseminated cerebral histiocytosis X responding to vinblastine therapy: a case report. Brain Dev 13:193–195
4. Idbaih A, Hoang-Xuan K; Martin-Duverneuil N, Genereau T, Thomas C, Barthez MA, Donadieu J, and The French LCH STUDY GROUP (2004) Langerhans Cell Histiocytosis presenting with progressive cerebellar ataxia: a clinical and neuroradiological study of 13 cases. Neurology 62 (Suppl 5): A196–A197
5. Martin-Duverneuil N, Idbaih A, Hoang-Xuan K, Donadieu J, Genereau T, Guillevin R, Chiras J, and the French Langerhans Cell Histiocytosis Study Group (2006) MRI features of Neuro_degenerative Langerhans Cell Histiocytosis. Eur Radiol 16:2074–2082
6. Prayer D, Grois N, Prosch H, Gadner H, Barkovich AJ (2004) HMR imaging presentation of intracranial disease associated with Langerhans cell histiocytosis. AJNR Am J Neuroradiol 25: 880–891
7. Barthez MA, Araujo E, Donadieu J (2000) Langerhans Cell histiocytosis and the central nervous system in childhood: evolution and prognostic factors. Results of a collaborative study. J Child Neurol 15:150–156
8. Grois N, Prayer D, Prosch H, Lassmann H (2005) Neuropathology of CNS disease in Langerhans cell histiocytosis. Brain 128:829–838
9. Grois NG, Favara BE, Mostbeck GH, Prayer D (1998) Central nervous system disease in Langerhans cell histiocytosis. Hematol Oncol Clin North Am 12:287–305
10. Grois N, Barkovich AJ, Rosenau W, Ablin AR (1993) Central nervous system disease associated with Langerhans' cell histiocytosis. Am J Pediatr Hematol Oncol 15:245–254
11. Wells WM, Viola PV, Atsumi H, Nakajima S, Kikinis R (1996) Multi-modal volume registration by maximization of mutual information. Med Image Anal 1:35–51
12. Pluim JPW, Maintz JBA, Viergever MA (2003) Mutual information based registration of medical images: a survey. IEEE Trans Med Imaging 22:986–1004
13. Calming U, Bemstrand C, Mosskin M, Elander SS, Ingvar M, Henter JI (2002) 18-FDG PET scan in central nervous system Langerhans cell histiocytosis. J Pediatr 141:435–440
14. Birnbaum DC, Shields D, Lippe B, Perlman S, Phillipart M (1989) Idiopathic central diabetes insipidus followed by progressive spastic cerebral ataxia. Report of four cases. Arch Neurol 46: 1001–1003
15. Poe LB, Dubowy RL, Hochhauser L, et al. (1994) Demyelinating and gliotic cerebellar lesions in Langerhans cell histiocytosis. AJNR Am J Neuroradiol 15:1921–1928
16. Polizzi A, Coghill S, McShane MA, Squier W (2002) Acute ataxia complicating Langerhans cell histiocytosis. Arch Dis Child 86:130–131
17. Manning L, Sellal F (2003) Hypothalamic amnesia and frontal lobe function disorders after langerhans cell histiocytosis. J Neurol Neurosurg Psychiatry 74:1348
18. Nanduri VR, Lillywhite L, Chapman C, Parry L, Pritchard J, Vargha-Khadem F (2003) Cognitive outcome of long-term survivors of multisystem langerhans cell histiocytosis: a single-institution, cross-sectional study. J Clin Oncol 21:2961–2967
19. Whitsett SF, Kneppers K, Coppes MJ, Egeler RM (1999) Neuropsychologic deficits in children with Langerhans cell histiocytosis. Med Pediatr Oncol 33:486–492
20. Otsuka M, Ichiya Y, Kuwabara Y, et al. (1996) Glucose metabolism in the cortical and subcortical brain structures in multiple system atrophy and Parkinson's disease: a positron emission tomographic study. J Neurol Sci 144:77–83
21. Foster NL, Gilman S, Berent S, Morin EM, Brown MB, Koeppe RA (1988) Cerebral hypometabolism in progressive supranuclear palsy studied with positron emission tomography. Ann Neurol 24:399–406
22. Buchler T, Cervinek L, Belohlavek O, et al. (2005) Langerhans cell histiocytosis with central nervous system involvement: Follow-up by FDG-PET during treatment with cladribine. Pediatr Blood Cancer 44:286–288